

A - A VIEW IN THE INVISIBLE

Slavica Ristić

*doi:10.2298/TAM1301087R Math. Subj. Class.: 76-05; 76E09; 76E30; 78-05.

According to: *Tib Journal Abbreviations (C) Mathematical Reviews*, the abbreviation TEOPM7 stands for TEORIJSKA I PRIMENJENA MEHANIKA.

A - A VIEW IN THE INVISIBLE

UDC 531; 534; 517.944;

Slavica Ristić

Institut Goša, Milana Rakića 35, Belgrade

Abstract (bold). *Flow visualization is an important topic in, experimental and computational fluid dynamics and has been the subject of research for many years. This paper presents an overview of flow visualization techniques. The physical basis and applications of different visualization methods for subsonic, transonic and supersonic flow in wind and water tunnels are described: direct injection methods, (smoke, dye, fog and different small particles), gas and hydrogen bubbles, , flow visualization by tufts, oil, liquid crystals, pressure and temperature sensitive paints, shadow, schlieren, interferometry, Laser Doppler Anemometry, Particle Image Velocimetry and other special techniques. Almost all presented photos have been recorded during tests in laboratories of MTI Belgrade.*

Key words: *flow visualization, wind tunnel, water tunnel, optical methods, LDA, PIV*

1. INTRODUCTION

Most fluids are transparent media and their motion remains invisible to the human eye during direct observations. However, the motion of such fluids can be recognized using techniques by which the flow is made visible. Such techniques are called flow visualization techniques. These techniques are valuable tools in various scientific and engineering disciplines. They allow to see the invisible: the optical inhomogeneities and motion in transparent media like air and water.

Flow visualization probably exists as long as fluid flow researches itself and dates back to the mid - 1400's, where Leonardo De Vinci sketched images of fine particles of sand and wood shavings which had been dropped into flowing liquids. Ludwig Prandtl, one of the pioneers of aerodynamics in Göttingen, performed first qualitative visualization of unsteady flows behind profiles and other models in his simple water channel by observing the movement of tracer particles on the surface of the water. Today, one hundred years later, most physical quantities of interest to mechanics,

aerodynamics and hydrodynamics can be determined quantitatively by image based experimental techniques. Modern image based measurement techniques such as Particle Image Velocimetry, following the same simple physical principles.

The progress made with optoelectronics and computer, lasers, video techniques has stimulated the development of a great number of image based measurement techniques. These techniques are now utilized for fundamental research, in industrial applications and for comparison with the results of numerical calculations. They allow a much better understanding of complex unsteady flow phenomena and providing quantitative information about the complete flow field [1-6].

Experimental flow visualization techniques are applied to get an picture of fluid flow around a real object or a scaled model of object, without any calculations and to develop or to verify new models and new theories of fluid flow.

If the flow could be made visible by some kind of flow visualization technique, then it would be possible to observe flow phenomena e.g., vortex flows, flows distant from surfaces, as well as those phenomena which are dominated by the effects of viscosity, e.g., boundary layer flows, separation) [1-41].

Flow visualization may be divided into surface flow visualization (tufts, fluorescent dye, oil or special clay mixtures) and off-the-surface visualization (tracers as smoke particles, oil droplets or helium-filled soap bubbles). Surface flow visualization gives important information on such things as the state of the boundary layer (laminar or turbulent), transition, flow separation and so on. The second type of visualization gives the information about whole flow field. Each of these methods requires appropriate lighting and some device for recording the image such as a still or video camera. Flow visualization offers integration of photographic art and engineering techniques.

Recently a new type of visualization has emerged: computer-aided visualization. In the area of fluid dynamics, computers are extensively used to calculate velocity fields and other flow quantities, using numerical techniques to solve the Navier-Stokes equations. Usually, when data sets are computed that provide a huge amount of sampled vector information spread over a two or three-dimensional domain. Without visualization it is impossible to investigate such data sets. To analyze the results computer visualization techniques are necessary and very often used. Humans are capable of comprehending much more information when it is presented visually, rather than numerically.

Three basic types of experimental techniques can be distinguished: methods with **adding foreign material**, **optical methods** and **methods with adding heat/energy**. **According with these principles**, one possible classification of the flow visualization techniques may be:

I Non optical methods:

1. Visualization with tracers (photochemical production of tracers, elektrochemical production of tracers, injection of tracers, smoke, dye, air and hidrogen bubbles, powder, fog and so on)
2. Surface visualization (tufts visualization (ordinary tufts, fluorescent tufts), oil emulsion, liquid cristals, termo sensitive paint, pressure sensitive paint, clay mixture)

II Optical methods:

1. Shadow method

- 2.Schlieren metod (paralel or focused, gray or color)
 - 3.Interferometry (classical, holographic)
 - 4.Electronic speckle interferometry and shearography
 - 5.Laser Doppler anemometry
 - 6.Particle Image Velocimetry
- III Special methods:
- 7.Energy adding
 - 8.Refractometry
 - 9.Laser light sheet

This paper reviews flow visualization techniques applied in wind and water tunnel tests. Wind tunnels are devices for experimental study of the wind effects on different structures or objects: aircraft and missiles models, vehicles, cars, bridges, buildings, machines, pipe and so on. But main task of the wind tunnels are experimental support of research and development during design phase of aircraft projects. The hydrodynamic behavior of submerged bodies in flowing water is studied in water tunnels, experimental facilities, where water is used as the working fluid [6,7].

Wind and water tunnels are equipped with modern instrumentation, making possible various measurements: force measurements on 3D models, half models or wing section (2D) models, simultaneously using external and internal wind tunnel balances, pressure distribution measurements, using Scanivalves, mechanical or electronically scanned pressure sensors, stability derivatives measurements, flow visualization, store loads measurements, hot film and hot wire anemometry, Laser Doppler anemometry, holographic interferometer, Schlieren systems, aerodynamic noise measurements and so on.

The flow visualization techniques used in aerodynamic laboratories of MTI [5,7], are: wall tracing method with pigment oil film (TiO₂, color pigments, graphite powder, lampblack, fluorescent dye) and liquid crystals, surface tuft methods with thin nylon or silk monofilaments and fluorescent mini tufts, smoke visualization techniques: smoke produced in smoke generator; smoke introduced at front of the test section and by vaporization of TiCl₄ for local application, water tunnel flow visualization by the use of gas bubbles, milk as tracer, aniline and methylene dye, aluminum powder and polystyrene particles, shadowgraphy, schlieren method, holographic interferometry, hot wire and hot film anemometry, Laser Doppler Anemometry.

2. TRACER METHODS

The visualization technique of streamlines, filament lines or particle paths, which injects some foreign material into a flow as a tracer is the most popular one and has been long and widely used up to the now. These three curves coincide if the flow field is stationary. But in the flow that depends on space and time as well, the three types of curves are different from one another. Which curves will be visualized depends on the choice of: where particles are introduced, the length of the exposure time, and the reference system from which the flow is observed or photographed. There is no difference between liquid and gaseous flows [1,2,5].

2.1. Smoke Visualization of the Flow

Recent developments indicate that smoke visualization in wind tunnels, one of the oldest flow visualization techniques, will continue as an important experimental tool in the study of complex flow dynamic phenomena. Improvements in generation and injection of smoke as well as in lighting (laser as a light source), in technique of acquisition and computation have continued to increase the scientific value of this method [1-5,9]. The similar results give the flow visualizations with fog and vapor.

There exists no upper limit of speed for smoke line visualization.

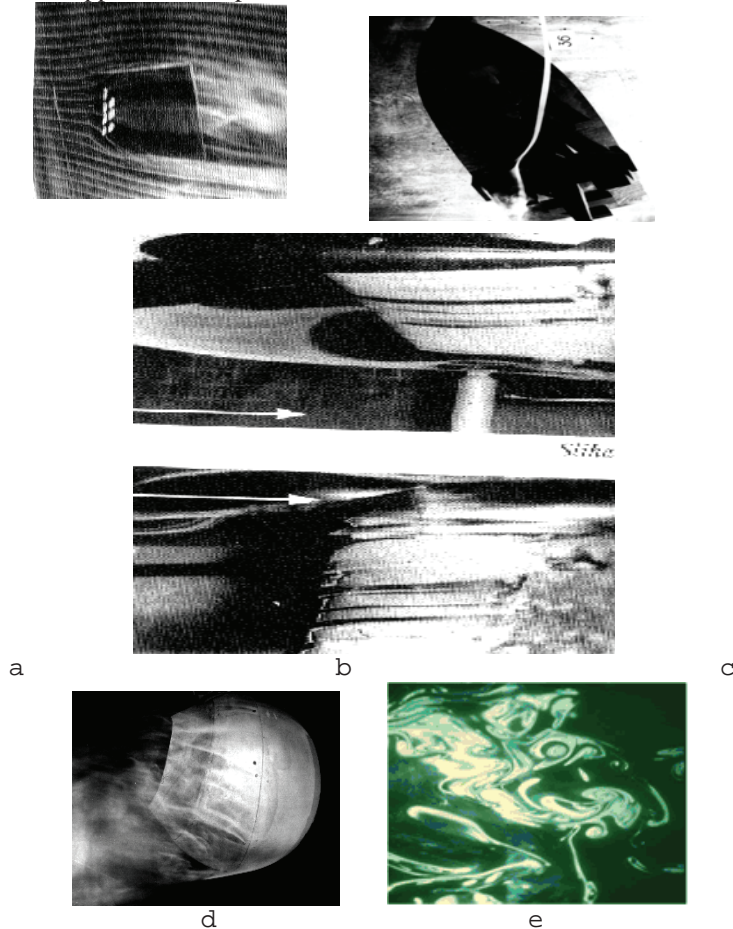


Fig. 1: Flow visualization in the MTI wind tunnels by different type of smoke.

Smoke line can be generated in a wind tunnel by introducing smoke (produced by smoke generated devices [1]) through small pipes placed in front of a test model, or through holes on the model surface. The smoke must be dense and white for visibility, no toxic, and no corrosive. The quality of the observed or photographed smoke line depends also on the choice of the illumination system. The smoke can be obtained by the vaporization of a mineral oil (paraffin, kerosene) mist resulting from the vaporization of certain

substances containing bromide or chloride, and smoke from burning or smoldering wood, paper, or tobacco. The burning or vaporization is done in a smoke generator. The flow visualization without smoke generator is possible if one deposits a drop of TiCl_4 (titanium tetrachloride) or $\text{C}_{10}\text{H}_7\text{Br}$ (bromnaph-thalin) onto the surface of test model in a wind tunnel, a white stream of smoke will originate from this drop. When the liquid TiCl_4 contact with the moist air develops powder TiO_2 and HCl . TiCl_4 liquid and vapor are corrosive and toxic because of HCl [5,9].

Fig 1. shows some examples of smoke visualization (flow is left to right): the smoke line in the MTI small smoke tunnel (fig.1a), visualization obtained with smoke introduced in the flow trough the ship chimney (Fig 1b), and flow visualization with TiCl_4 around airplane model and sphere (figs.1c and 1d), smoke and laser sheet visualization of turbulent convection patterns (fig.1e).

One of the more significant improvements in the filed of smoke visualization in the past several years has been the introduction of laser light illumination. By using a light sheet, cross section of the wake can be illuminated and the position of the vortices can be located (fig.1e). Unsteady flow can be tested with pulsed laser. Recording of the flow visualized effects can be affected by still or movie camera. Some times that method is classified as special flow visualization method [4,5,12].

2.2. Visualization using dye

The visualization of the liquid flow patterns by ejection of a dye is an analog of the smoke visualization technique[1-6,12,13]. The dye can be injected in a tested flow either from a small ejector tube placed at a desired position or from small orifices, that are provided in the wall of a model (fig.6a), without the component perpendicular to the model surface. It can be generated in the flow too, without disturbing the flow. The dye has to be stability with respect to diffusion, to have the same specific weight as the working fluid and high contrast.

For the purpose of flow visualization can be used the food coloring dyes, aniline, methylene, potassium permanganate, ink or fluorescent dyes (fluorescent rhodamine), mixing in milk or alcohol. The fattiness of the milk retards diffusion of the dyed solution into water and give high contrast of the dye line. In a rotating flow, it is important to have dye solution with the same specific weight as working fluid (mixing dye with alcohol).

The aniline violet, red and blue dye, injected from small orifices placed in the top of the model, in the cabin region, visualizes the flow around tested models (flow is left to right): 1/48 scale model of F-18 aircraft in flow visualization facility (ONERA, fig. 2a [9]) and in MTI water tunnel, fig 2b. Fig. 2c shows flow visualization around hydro profile in MTI water tunnel with aniline dye and fig 2d. is vortex visualization Karman vortex street behind a cylinder at increasing Re number, using fluorescent dye and laser sheet.

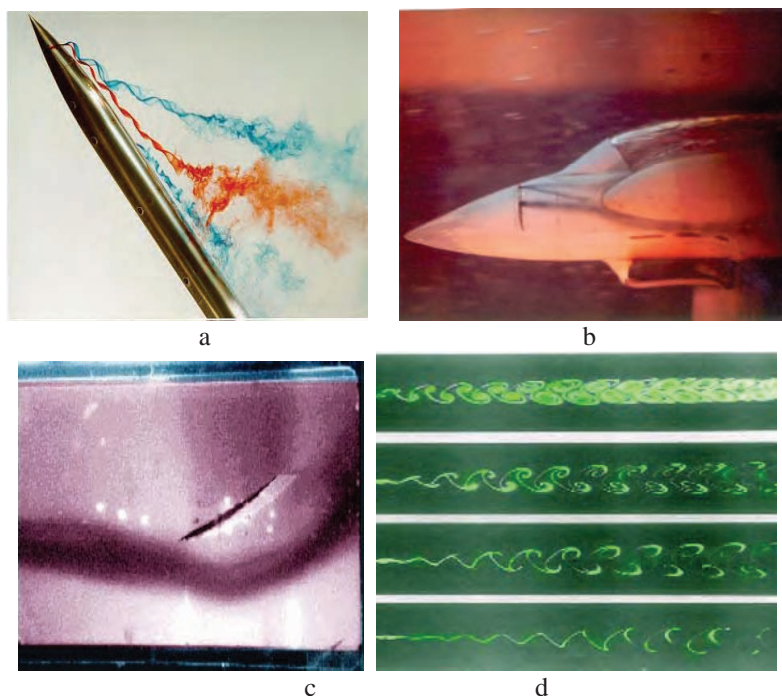


Fig. 2. Flow visualization by different dyes

The dye methods used in a closed circuit water tunnel increasingly contaminate the water. The tunnel has to be emptied and refilled after each experiment. Visualization with dye is not suited for turbulent flow, since the filaments would decay and the dyes would mix with surrounding fluid immediately after being ejected [1,3,5,9-12].

Electrolytic and photochemical reactions can produce different dye in aqueous solutions, which allows flow visualization and velocity profile measurements. Focusing light from a flash tube or pulsed ruby laser onto a point in the photoactive solution fluid (pyridine dissolve in ethyl alcohol or nitrospyran in kerosene) initiates a photochemical reaction, which yields a spot of blue dye within a few microseconds [1].

2.3. Visualization by different small particles

Adding small particles in the flowing flow (water or air) supposed that the velocity of the particles and fluid are identical. The tracer particles can be either solid, liquid, or gaseous and the fluid liquid or gaseous, for example: dust, magnesium, (Mg), Al_2O_3 , TiO_2 , aluminum (fig. 3) and polystyrene or cosmetic powder, lycopodium, hostaflon, cigarette smoke, metaldehyde, atomized DOP, glass sphere, marble dust, oil drops, water drops, hydrogen, gas, helium bubbles, ...The diameter of the particle is between 0.1 to 20 microns [1,4,5].

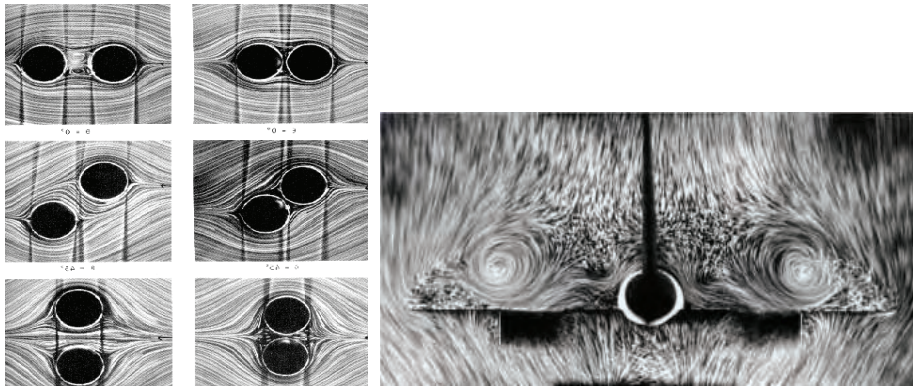


Fig. 3. Visualization the flow around two cylinders (a) and moiled of Concorde with Al powder (ONERA)[1,9]

For determining the trajectory and local velocity of a spherical particle, the equation of the motion of a single particle must be solved. It is necessary to complete the equation of the motion with gravity and "lift force" acting on the particle in the flow with velocity gradient. The particle velocity approaches exponentially the constant fluid speed. The approach is the faster, the density and the size of the particle are smaller. In the compressible flow, with shock waves, particles of finite mass and size cannot follow such an abrupt change of the state of motion. The used particles should be as small as possible, neither corrosive nor toxic and to have high degree of light reflectivity. The injection into the fluid should be located far enough upstream the test regime. In principle two methods exist; to take a single or multiple photographic exposure of the flow field with controlled exposure time or to take exposure of the flow field so that each moving particle is reproduced on the photograph by a single streak of finite length. Stereoscopic photos or holograms may overcome the problem of localization of the particle. Today there are a lot of different methods for illuminating and recording. [1,2,5].

Particle Image Velocimetry (PIV) is an experimental method for indirectly flow visualization but method providing directly, instantaneous velocity vector measurement in a cross section of a flow. The method is classified as special method or as the flow visualization method by small particles. The basic principle involves photographically recording the motion of microscopic particles that follow the fluid flow [5,13]. The technique is ideal for unsteady aerodynamic flows. The software for PIV is a visual programming language combining complete control of the acquisition, redaction and analysis. The application of PIV method is illustrated with example presented in figure 4. The measured velocity distributions performed by PIV image of the flow with the Mach-4.5, on the upper part of the 20°- half angle wedge with flow is left to right (fig.4a) is shown in Figs. 4b and 4c for the horizontal and vertical velocity component, respectively.

Laser Doppler Anemometry (LDA) is optical technique for investigation of velocity and turbulence in gas, liquid, and mixing fluids, flame, rotating machinery, in combustion, channels, chemically reacting flows, wave tanks wind or water tunnels, in biomedical applications, atmospheres, oceanography and in various spectrum of scientific and industrial research. LDA is power fool method for indirect flow visualization, too[11,14,15]. The basic idea underlying LDA is to measure the velocity of

tiny particles transported by the flow. If these particles are small enough, their velocity is assumed to be that of the stream and LDA provides a measure of the local instantaneous velocity, the mean velocity as well as the turbulent quantities.

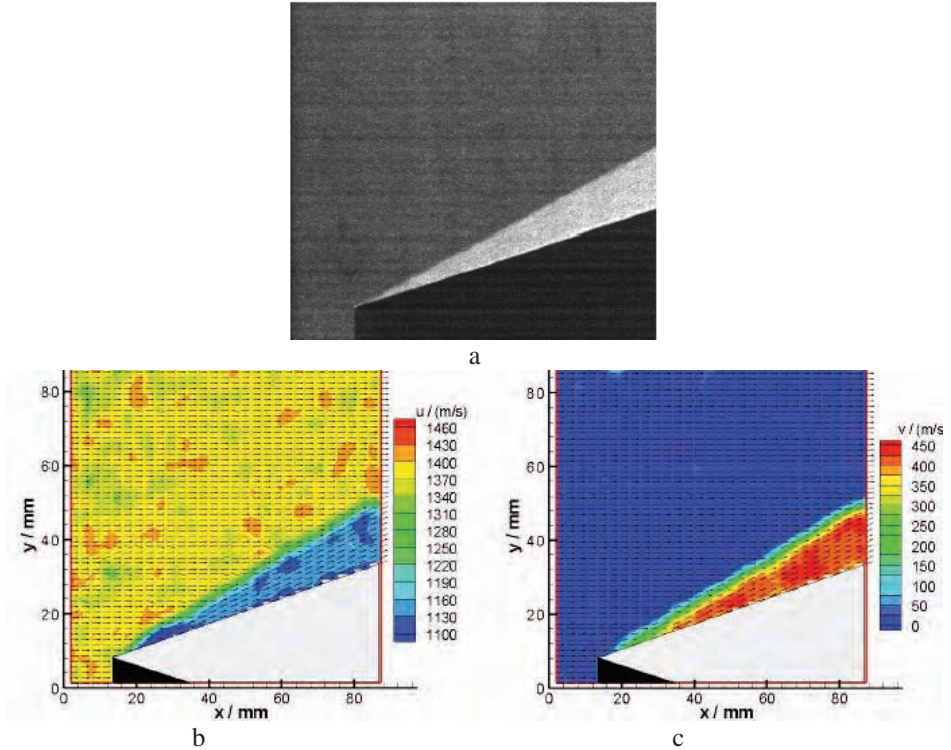


Fig. 4. (a) PIV image of wedge, (b) horizontal flow velocity, (c) vertical flow velocity [13]

Laser anemometers offer some advantages in comparison with other fluid flow instrumentation: non-contact optical measurement. LDA probe the flow with focused laser beams and can sense the velocity without disturbing the flow in the measuring volume, non calibration – no drift. The laser anemometer has a unique intrinsic response to fluid velocity—absolute linearity, well-defined directional response. The quantity measured by the LDA is the projection of the velocity vector on the measuring direction defined by the optical system, high spatial and temporal resolution, multi - component and multi - directional measurements and so on.

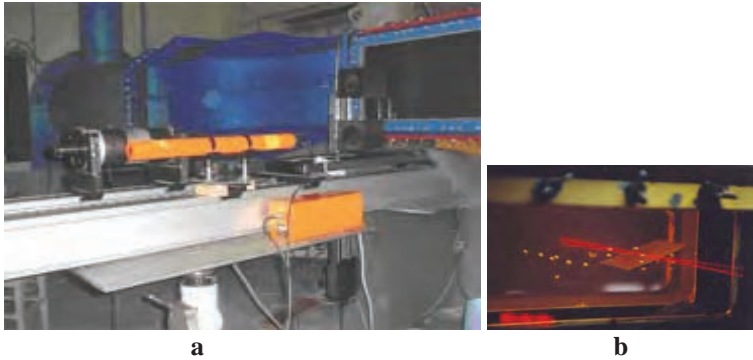


Fig. 5: Some details of experimental setup, a) water tunnel and 1D LDA, b) hydrofoil in WCT test section and laser beams[11]

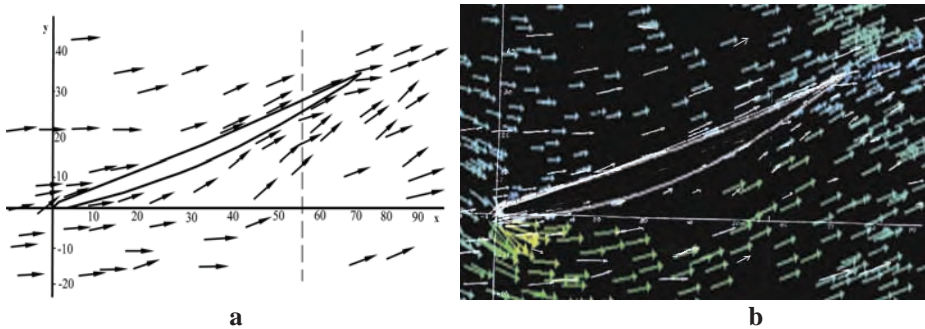


Fig. 6: LDA, experimental (a) and numerical (b) results of visualization by vector velocity distribution for flow around hydrofoil positioned at $\alpha = 25^\circ$, $V_\infty = 5.32$ m/s, (flow is left to right)[14]

2.4. The gas bubble visualization

Gas bubbles visualization is a tracer method where tracer particles have low (in the water), or similar density (in the air) as the flow. The observation of such gaseous tracers in a gaseous flow requires the use of optical visualization methods. The gas bubbles change its shape during the motion, and as a consequence, the drag coefficient of these gaseous tracer particles is not only a function of the velocity difference between fluid and particle, but also a function of the deforming forces acting on the particle. The gas bubbles can be injected in the flow or generated by electrolysis [1, 5].

In a conventional arrangement hydrogen bubbles are produced on the cathode. They mark a line of fluid elements whose position coincided at a given instant with the position of wire. Any later position of these rows of tracer particles is called a "time line", that is a measure of the local velocity profile (fig.7a), while fig 7b shows co-rotating vortices and saddle points upstream of a bluff protuberance mounted on a flat plate (flow from top) visualized by hydrogen bubbles and laser sheet flow visualization in a water tunnel.

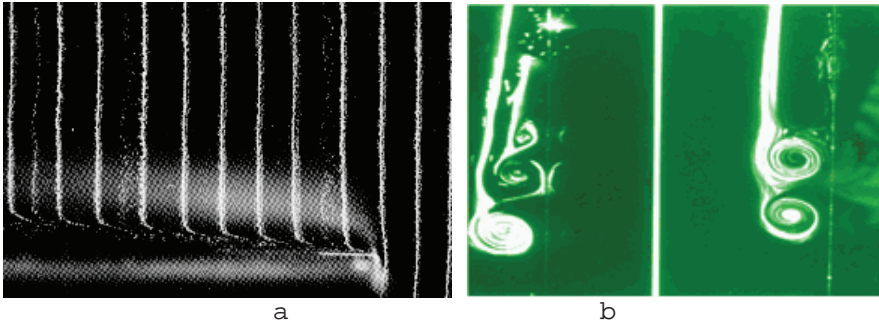


Fig. 7. Rows of the hydrogen bubbles indicate the velocity profile over the plate [1] and co-rotating vortices

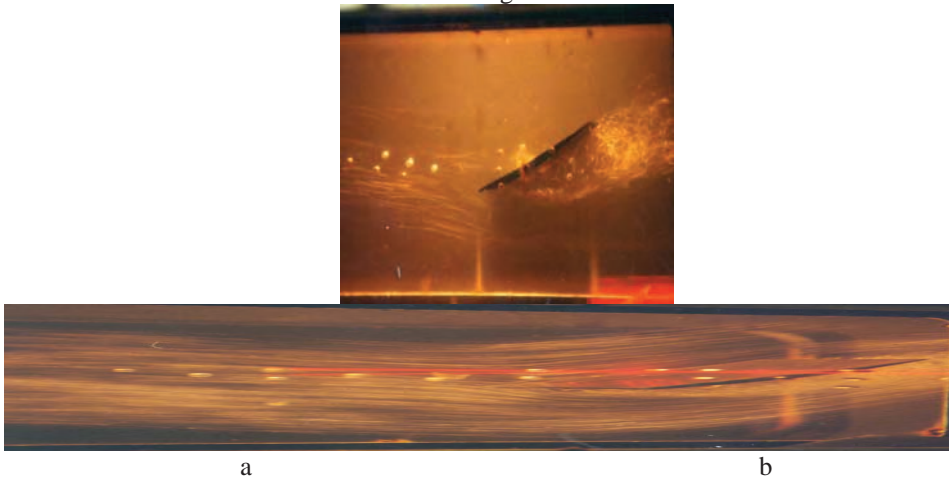


Fig. 8: Flow visualization in MTI water tunnel with air bubbles around hydrofoil with different quantity of injected air [11]

The bubble motion can be recorded with a still or move camera. Time of observation bubbles in the flow is limited by the dissolution of the gas bubbles in the fluid (in water the time is approximately 3 s). The application of this method is limited in the laminar, low speed flow [2,3]. Fig.8 shows the flow around hydrofoil in the water tunnel (MTI) visualized by air bubbles [11].

3. FLOW VISUALIZATION BY TUFTS

Very frequently, flow visualization in the vicinity of model, in subsonic flow, is performed using tufts. [1-5,16-18]. However, tufts size, their distribution on the model surface and sticking are important for turbulent flow testing and for higher quality boundary layer visualization on complex models. A grid with attached or glued tufts as a

screen can be used to visualize the vortex shedding behind model or in the interaction regime of different field. [2].

Fluorescent tufts have numerous advantages in comparison with the ordinary silk tufts [1, 5, 16-18]. By using fluorescent dyes, the tuft diameter virtually increases as well as the illumination, thus allowing higher quality of recording and using thinner tufts (0.01-0.1 mm). They can be stuck onto the model surface using very small glue quantities, (0.04 mm), thus avoiding boundary layer disturbances. Strong centrifugal forces interfering with flow field act on tufts stuck onto the model surface and their resultant determines tuft orientation.

The problem with small size diameter is overcome by using light source with rich ultraviolet part of the spectrum, or special filters transmissible to that part of the spectrum. This increases tuft luminance making it look much thicker and brighter. Hg or Xe lamp with UV filters for $\lambda = 350$ nm are used for steady flow testing. Stroboscopic light sources are most frequently used for unsteady flow. Fluorescent tufts are also used for flow visualization in water tunnels, as well as in-flight flow testing.

Figure 7 demonstrates the results of experiment in subsonic wind tunnel; flow visualization with fluorescent silk tufts. The light combat aircraft model has surface painted in opaque black with 840 tufts stick on it. Tufts are made of silk 0.05 mm and 20 mm long (figure 9a). Fluorescent spray was used for tufts dying. The flow speeds have been between 20 and 40 m/s, and angle of attack has been altered from -8 to $+24^\circ$. UV lamp with 100 W has been used as light source.

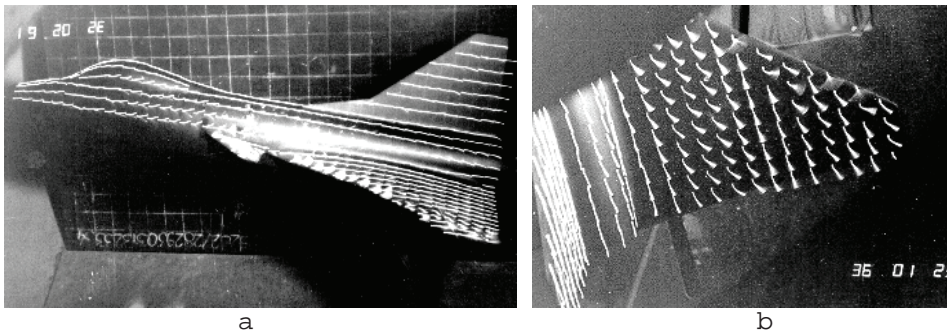


Fig. 9: Flow visualization with fluorescent tufts in subsonic wind tunnel (flow is left to right)[18]

4. SURFACE FLOW VISUALIZATION METHODS

For observation of flow characteristics close to the wall of a model, the body wall can be coated with a certain material which indicates the local wall temperature, surface pressure, or the streamline pattern of flow adjacent to the wall [1-5,19-22].

4.1. Surface Oil Film

Oil film or dots on the model surface enable one to quickly and easily obtain a picture of flow pattern at the surface of the model placed in wind tunnel [1-5,]. The special mixture can be prepared of appropriate oil and a fine pigment (Al_2O_3 ; TiO_2 , powder, fluorescent dye, coloring pigments, and graffito). The technique allows observation the lines of separation and reattachment of the flow at the body.

Fig. 10a and 10b shows the visualization with $\text{TiO}_2 + \text{oil}$ on the surface around two and three vertical cylinders fixed on the plate in subsonic wind tunnel for $V=50 \text{ m/s}$ and around sphere used for turbulence test for $M=0,2$ (fig. 10c)[5,22]. Figure 10d is oil flow visualization of the airflow on end wall of a turbine blade cascade. Boundary layer flow visualization on the laser guided bomb model with oil film, performed in the large trisonic wind tunnel, top of the model with fins (a) flow on the fin upper surface (b), on the wing upper surface (c) for $M_\infty=0.9$ is presented on fig. 11.

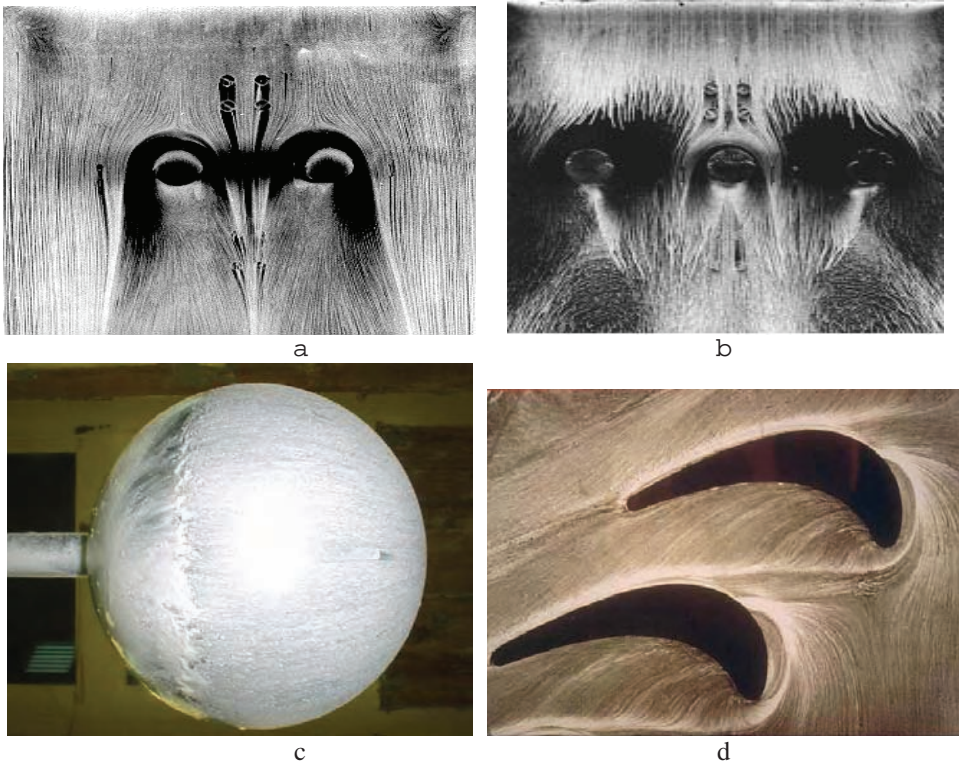


Fig. 10: Flow visualization around two (a) and three (b) cylinders fixed on plate in large wind tunnel T-35 for $M=0,5$ with oil film, around sphere for $M=0,2$ (c) [9] and airflow on end wall of a turbine blade cascade [25].

Test of the flow field around the axisymmetrical body – model of the torpedo without fins and control surfaces, was performed in the trisonic wind tunnel T-38 of MTI, for the speed of undisturbed flow which corresponds to Mach number $M_\infty=0.3$.

Aerodynamic forces and moments were measured by six-component internal strain gage balance. Oil emulsion film with addition of oleic acid and TiO_2 powder was used for flow visualization in the boundary layer (fig. 23)[20-23].

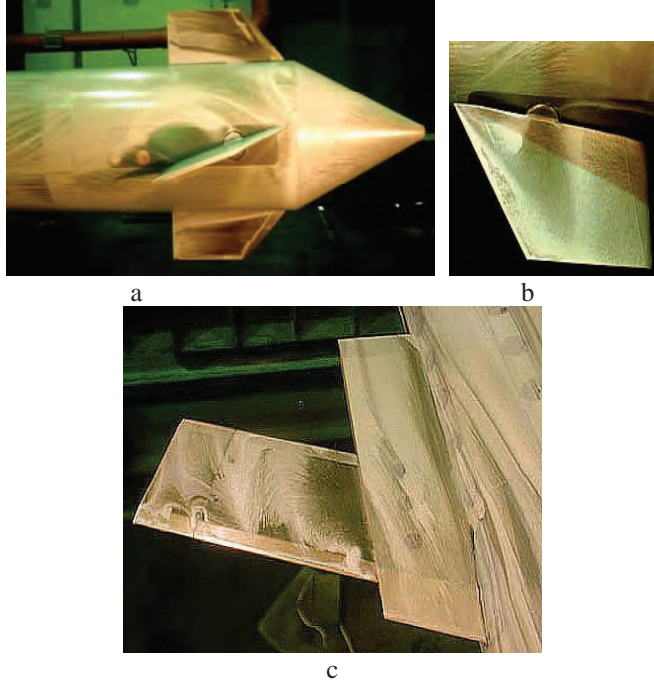


Fig. 11. Boundary layer flow visualization on the laser guided bomb model with oil film, top of the model with fins (a), flow on the fin upper surface for $M_\infty = 0.9$ (b) and flow on the wing upper surface (c)[19].



Figure 12: Flow pattern on the model obtained by the experiment (a) and by the simulation of the flow for $M_\infty = 0.3$ and $\alpha = 8^\circ$ (side view) (b) [21].

The goal of the experiment was to make possible comparison of the aerodynamic coefficients and flow pattern obtained by the experiment and by the simulations of the flow. Fluent 6 was used for simulation of the flow. Analysis of shown photographs (figure 12a and 12b) demonstrates an excellent agreement of flow patterns obtained by the experiment and the numerical simulations.

4.2. Liquid crystals and temperature sensitive paints

A surface-temperature distribution can be gained by coating a test model with cholestric liquid crystals. [1,2,5]. If they are illuminated with white light under a certain angle of incidence, then liquid crystals reflect only one light wavelength at each viewing angle, depending of small temperature changes in the crystals sheet. The colors of liquid crystals are reversal if the temperature changes in the opposite direction. Because of that, liquid crystals are very attractive for boundary-layer studies. Model to be tested should be made of a material with low heat conductivity and coated with black paint as base. Fig 13 demonstrates the application of liquid crystals for hot streams visualization in a subsonic wind tunnel.

The surface temperature, the local heat transfer rate and coefficient on a body tested in high speed flow facility can be measured by means of temperature sensitive paints. The important difference between liquid crystals and temperature sensitive paints is, that the temperature span over that liquid crystals change colors is much smaller (a few degrees only) than that of paints (several hundred degrees).

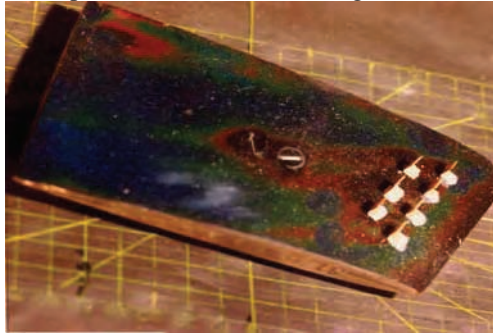


Figure 13: Flow visualization in small wind tunnel with liquid crystals [5]

4.3. Pressure sensitive paint (PSP)

The spatially continuous pressure and temperature distributions on aerodynamic test surfaces is important for understanding complex flow mechanisms and for comparison with predictions of computational-fluid-dynamics models [5,26]. Conventional pressure measurements are based on pressure taps and electronically scanned transducers. Pressure taps provide pressure information only at discrete points.

PSP technology is an alternative for determining static and transient surface-pressure fields for aerodynamic applications and for flow visualization. The pressure sensitivity is based on the oxygen (O_2) quenching of luminescent molecules dispersed in a film that is coated onto a test surface. In practice, the PSP/TSP (temperature sensitive paint) coating is illuminated with light of the appropriate energy (color) to excite the coating-entrapped probe molecules. The resulting luminescence output is inversely proportional to the surface pressure or temperature of the test model.

The output of the CCD array can be visually represented as a two-dimensional image, with the luminescence corresponding to a gray or false-color scale. Figure 14 represents the illustration for PSP applications.

5. FLOW VISUALIZATION WITH SPECIAL TECHNIQUES

Third group of visualization methods is based on two principles: introducing a foreign invisible substance into the incompressible flow, and visualizing the density variations in flow by optical methods. The foreign substance in this case is energy transferred to certain portions of the flow that increase energy level (spark, electron beam and glow discharge methods) and make artificially density variations. Such portions of the flow have an altered density and can be visualized by the optical methods.

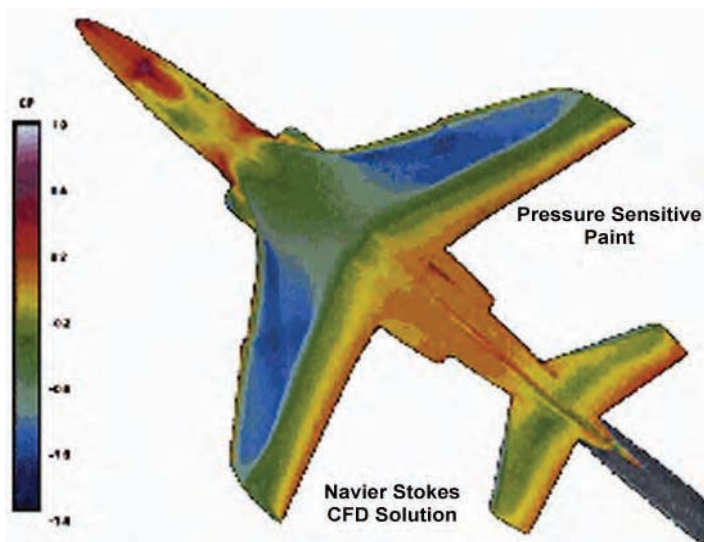


Fig. 14. A comparison of pressure results between PSP (right side of model) and Computational Fluid Dynamics (left side)[26]

They are applied to visualize the rarefied gases that are for several reasons distinguished from the ordinary compressible flows [1]. A technique which can be used even for very low density fluid flows is electron-beam flow visualization. A beam of electrons traverses the gaseous fluid. When electrons collide with gas molecules, these gas molecules will be excited and emit radiation. The intensity of the radiation is approximately proportional with the density of the fluid. By moving the electron beam, the entire flow area can be scanned (fig.15).

An intensive hot spot can be obtain by means of a spark discharge across two electrodes into a gas stream or using a giant pulse laser for producing the luminous plasma (Q-switched giant pulse ruby laser of 100 MW). Another way of artificially introducing density changes in a flow is to seed the flow with a foreign gas of different refractivity (benzene vapor, CO₂).

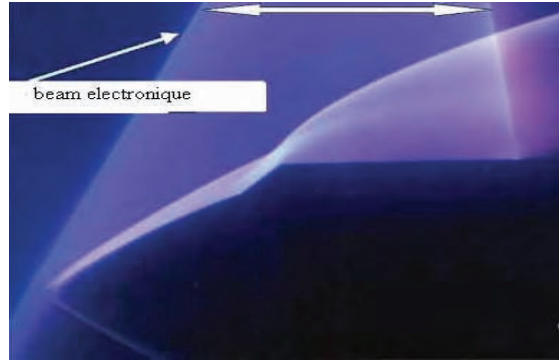


Fig. 15: Flow visualization by electronic beam in hypersonic wind tunnel for $M= 10$ [5]

Very often as special flow visualization techniques are mentioned methods where the double refracting liquids, solutions or suspension of certain macromolecules in a neutral solvent, are used. A transparent medium can be birefringent if it consists of optically anisotropic molecules.

For the purpose of flow visualization high speed photographic techniques are usually applied in connection with one of the visualizing method. High speed cameras with exposure time of 10^{-6} to 10^{-9} s in connection with associated illumination systems can record the shock wave motion.

6. COMPRESSIBLE AIR FIELD AS AN OPTICAL OBJECT

Airflow around aerodynamically models, in optical sense, is a transparent environment with complex light refraction index. Light refraction index n in each point is the function of air density, which, on the other side, is the function of speed, pressure and air temperature [1,5,27-37]. The relation between air density $\rho(x,y,z)$ and refraction index $n(x,y,z)$ is the Gladstone-Dale: $n = 1 + K\rho$. The constant K has dimension of ρ^{-1} and it is different for each gas.

According to Snell's law [1,3,5,27], a light ray, passing through inhomogeneous refracted field, is deflected from its original direction and a light path is different from that of undisturbed ray. If recording plane is placed in front of light ray, after disturbing media, three quantities can be measure: the vertical displacement of disturbed ray, the angular deflection of disturbed ray with respect to the undisturbed, the retardation of deflected ray, i.e. the phase shift between both rays [1].

Optical visualization methods are based on the recording one of these three quantities, or a combination of them. Shadowgraph used the first phenomenon, the Schlieren the second, and interferometry the last. The shadowgraph is sensitive to changes of the second derivative of density or refractive index $\partial^2 n / \partial y^2$, Schlieren to changes of density first derivative $\partial n / \partial y$, and the interferometry is capable to measure

absolute density n changes. If, using the optical method, light refraction index $n(x,y,z)$ in flow is determined, another physical parameters of tested environment, significant to aerodynamic testing, can be indirectly determined as well.

6.1. Shadowgraph method

The oldest and the simplest of all optical methods for flow visualization is shadowgraph [1-5].

Figure 16a shows the bow shock wave ahead of sphere in supersonic wind tunnel T-36 at $M_\infty = 1.86$ [5,7]. The trace of the shock wave on the photo is a band of absolute darkness bounded on the downstream side by an edge of intense brightness. The exact geometrical position of the shock front is the other edge of the dark zone. The shock wave represents a jump of the refractive index. The air density increases after the shock and the incident ray deviates to inside edge.

Since the density in the disturbance is lower than in the surrounding field, (Prandtl-Meyer expansion fan at the sharp end of the nozzle) the bright band appears at the beginning of the shadow [1-5,27]. The same result is obtained when the compressible boundary layers is visualized. Figure 16b is typical shadowgraph showing flow around spherical tipped cylinder mounted on flat plate [5].

Shadowgraph methods with short duration light pulses can be used for fine visualization of turbulent compressible flow.

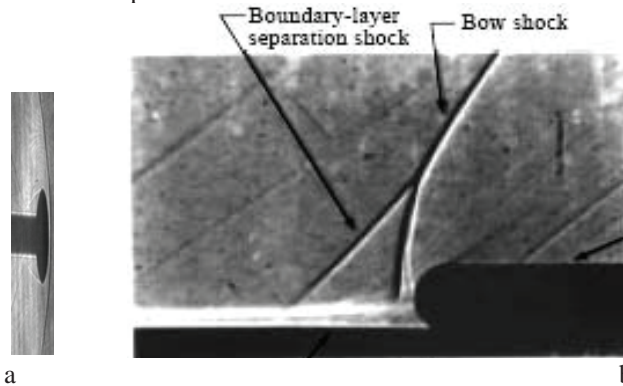


Fig. 16: Shadowgraph visualization around sphere (a), and typical shadowgraph images showing spherical tipped cylinder mounted on flat plate (b) [5]

6.2. Shlieren method

As is mention before, Schlieren method is sensitive to change of the first derivative of density $\partial n / \partial y$, (or refractive index) and it can record the angular deflection of the disturbed ray with respect to the undisturbed in a transparent medium with local inhomogeneities [1-5,27,32,33,36,37].

The Schlieren method is the most frequently used in aerodynamic laboratories, since it is relative simple and very useful method. If a parallel beam of light passes

through air with density gradient normal to the direction of the beam, the beam is refracted towards the region of greater density.

The most simply is the Schlieren system with parallel light through the test section of the wind tunnel. Töepler system in hypersonic wind tunnel, as the base of all other systems, is illustrated in Fig 17. Detail description of the system is presented in references [5].

The modern schlieren system uses color filter or phase optical elements instead of the knife-edge, and have several parallel, transparent, colored strips (most often three colored sheets, red-blue-yellow or blue-green- red). The color filter can be consisted of four differently colored strips arranged in a square filter for visualize the grad n in two direction. If the flow is axis symmetric, complementary colors appear for the same event (compression or expansion) above and below the flow axis.

The recorded pure colors and color combinations are a measure for the local direction of density gradient in the test section. Figure 17 shows parts of schlieren systems in T-34 hypersonic wind tunnels in MTI [5,7].

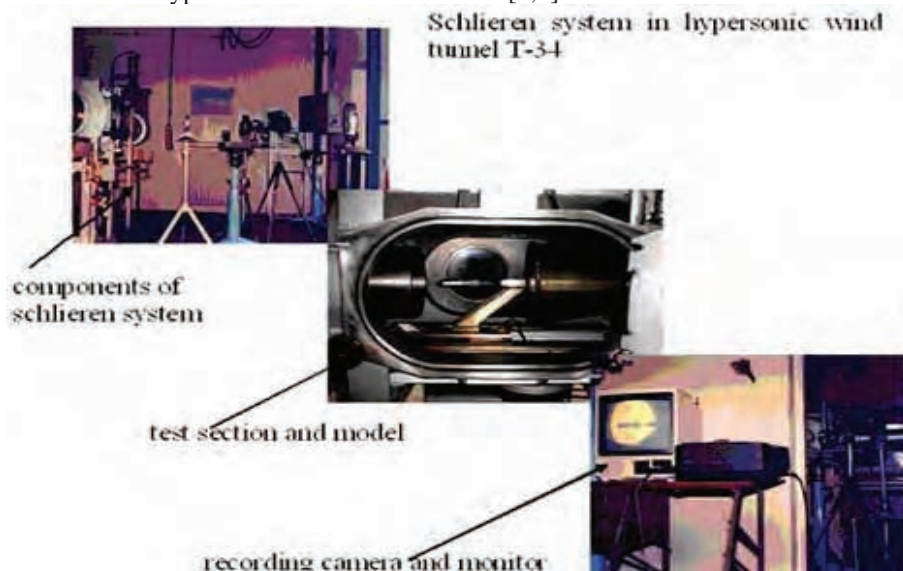


Figure 17: The photos of schlieren system components, model in the test section of hypersonic wind tunnel T-34 and TV camera with monitor

Attempts to increase the amount of information extractable from schlieren effects, the various opaque filters with different geometries, as well as transparent phase and color filters are used [1-5].

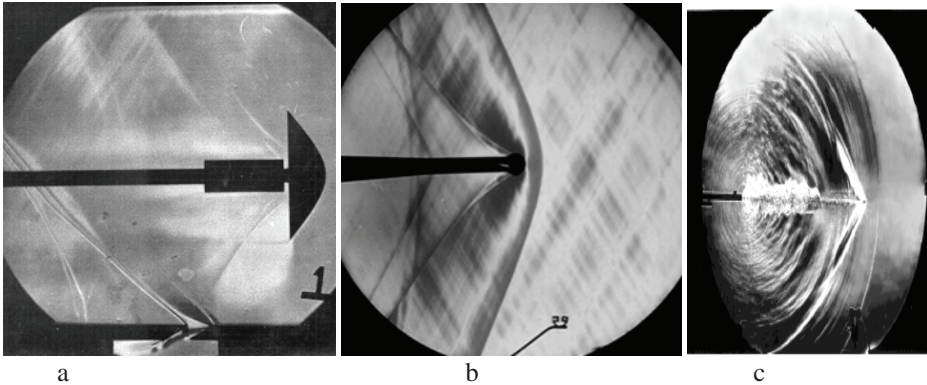


Fig. 18: Black and white schlieren in wind tunnel T-36 for $M_\infty = 0.86$ (a) and $M_\infty = 1,1$ (b), and instantaneous image of Bullet and Muzzle Blast from 22-Caliber Rifle (c)

Figure 19 shows color schlieren effects around blunt body and thin protruding probe mounted in front of a blunt body, used to reduce the drag and the rate of heat transfer, for $M_\infty=1.86$ [5,33]. Flow visualization in two dimensional model of the supersonic rocket nozzle without and with vertical, different height barriers is tested by schlieren method and the effects are presented in the fig 20. The nozzle is designed for Mach number in the output plane $M_\infty= 2.6$ [31,36,37].

The classical schlieren photos obtained with color schlieren system are presented in fig, 21. The flow around cone with top angle of 15° and sphere with $\Phi=40\text{mm}$ is tested in supersonic wind tunnel T-36 for different Mach number and position of color filters [5]

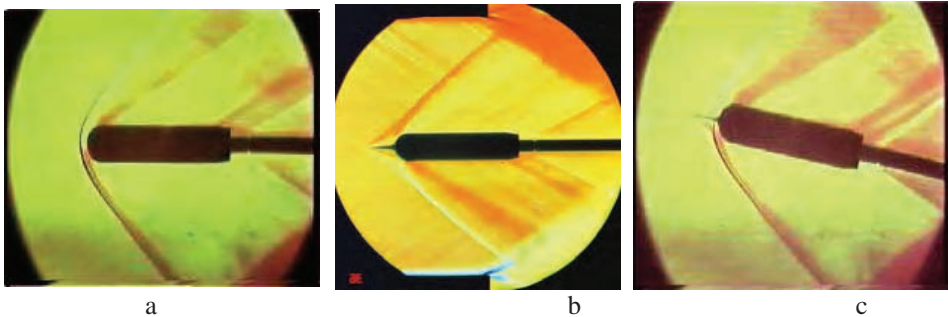
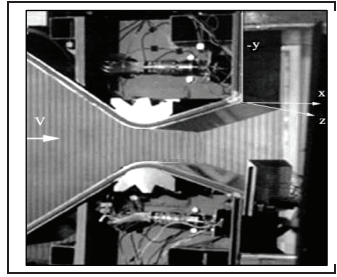
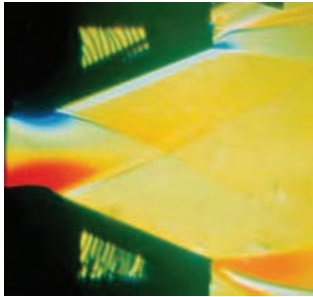


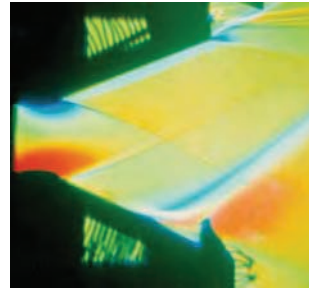
Fig. 19: Color schlieren effects around blunt body and thin protruding probe (flow is left to right)



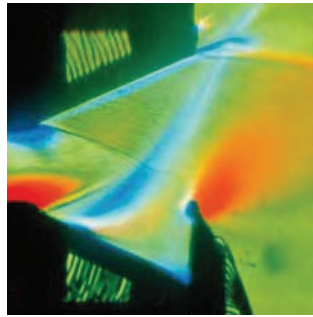
a



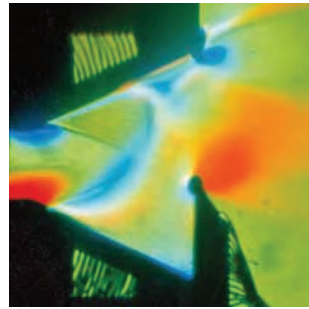
b



c



d



e

Figure 20 Schlieren visualization of the supersonic nozzle flow(flow is left to right)

The combined holographic interferometer and schlieren devices [5,35-37], have been designed, made and tested for small supersonic and large trisonic wind tunnel. The device can be included in tests either as schlieren system or interferometer.

Improvements to the basic schlieren system include the Rainbow Schlieren [1,3,5] where a colored bull's eye filter is used rather than a knife edge to quantify the strength of the refraction. The other variety of schlieren methods is obtained including laser as a light source. Figure 22 illustrates rezultats schlieren system in T-36 with He-Ne laser as a light source.

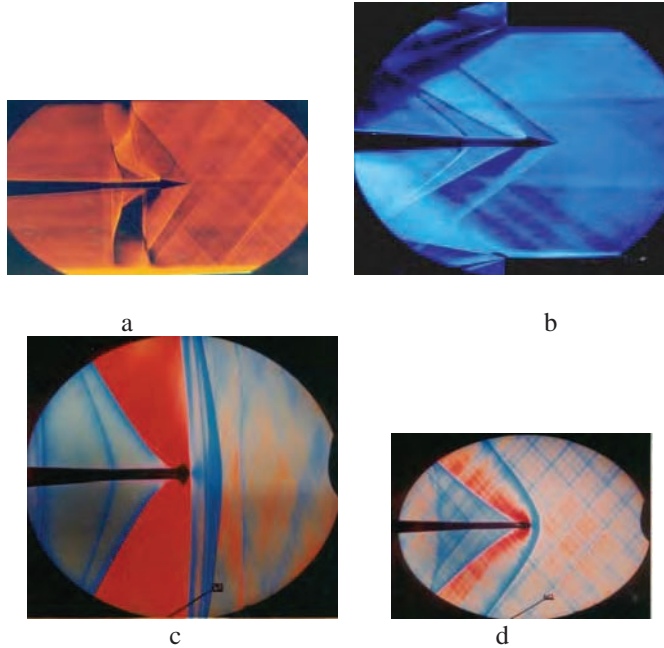


Fig. 21: Color schlieren photos obtained in T-36 wind tunnel for $M_\infty = 1.02$, and 1.56 around cone with 15 degrees top angle(a,b) and sphere with $\Phi=100\text{mm}$ (c,d) [5].

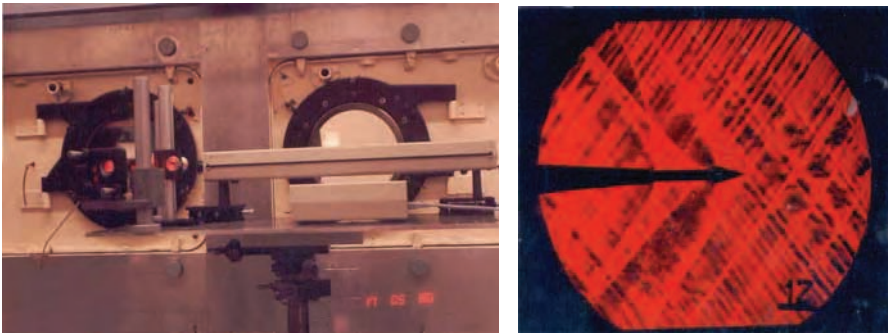


Fig. 22. Schlieren system with laser as light source in T-36 and schlieren effect around cone for $M_\infty = 1.1$ [5]

6.3. Interferometry

Interferometry is based on the fact that a change in density not only results in a refraction of the light, but also in a phase shift. In an interferometer parallel light is split into two beams. One of the beams enters the flow field, the other beam does not enter the flow field. When both beams are merged and projected on the same photographic plate, interference occurs when the phase of one of the beams is shifted by a change of density in the fluid flow [1-5,27-37].

The most used classical interferometer in the wind tunnel tests is Mach-Zehnder interferometer (MZI) [1,27]. MZI can be applied to any case of gas flow investigations, where density difference becomes noticeable as: thermodynamic data, thermal conductivity of gases, dissociation, aerodynamic application, turbulence, wave or sonic booms.

6.3.1. . *Holographic Interferometry*

Holographic interferometry is an optical method that makes possible complete flow field testing. The method is non-contact and it does not disturb flow field. It is used for testing of different object and phenomenon [1-5,27]. The greatest advantage of holographic interferometry, in relation to schlieren method, is the fact that it provides complete information stored in a single plate, allowing a postponement selection of specific types of flow visualization.

The base of this method is holography, developed in last forty five years [27]. If, on the some plate, the image of one object is recorded two times in different moments, in the process of reconstruction both images appear simultaneously and on the same place in the space. Object waves interfere because of mutually coherence (they originate from the same light beam that illuminate the hologram) and the interference effects can be observed in the reconstructed object image. If no change occurs on object between first and second exposition, then there is no difference in images and there are no interference fringes. If certain difference appears, then the reconstructed image contains the system of interference fringes N that indicate that change.

Quantitative flow testing, using holographic interferograms is performed by determining the number of fringes $N(x,y)$ in the field image with respect to a reference point of known density. After that, the index of light refraction $n(x,y)$ and the air density $\rho(x,y)$ can be calculated. For the isentropic flow, there existed relations between N , n , ρ , pressure P , temperature T , velocity V , and Mach number M . The physical base and mathematical interpretation of the holographic interferometry are explained in references

The simplest case for analyzis is the 2D flow [9,21,31-35]. For the processing of interferograms of axi-symmetrical phase objects, the method of inversion, based on the Abel transformation, is used. The experiment geometry is usually selected in order to simplify the mathematical representation of flow and changes occurring at the path of the laser light beam through the test section [5,29-32].

Computer tomography is an important technique for reconstructing 3-D fields from holographic interferograms [1,27-29]. Several techniques have been developed for computer tomography as: implicit methods (series expansion, discrete element representations), explicit methods (convolution method), and Fourier transform method. The choice of the best algorithm depends on structure of the density field, the amount and format of available data.

Holographic interferometer with parallel beams is at the same time schlieren and shadow device. Fig. 1 shows the schematic diagram of the experimental setup. Detail description of interferometer components is given in previous paper. During the experiments synchronized measurements were performed. Double exposition technique was used for holographic interferograms recording: wind off (when homogeneous flow

field exists) and wind on (when there is complex flow field for testing) [1,3,5]. Stagnation pressure (P_0), atmospheric pressure (P_a), and Mach number (M_∞) were measured by the primary measurement system (PMS) in the wind tunnel, at the moment of recording hologram, shadow and/or schlieren results.

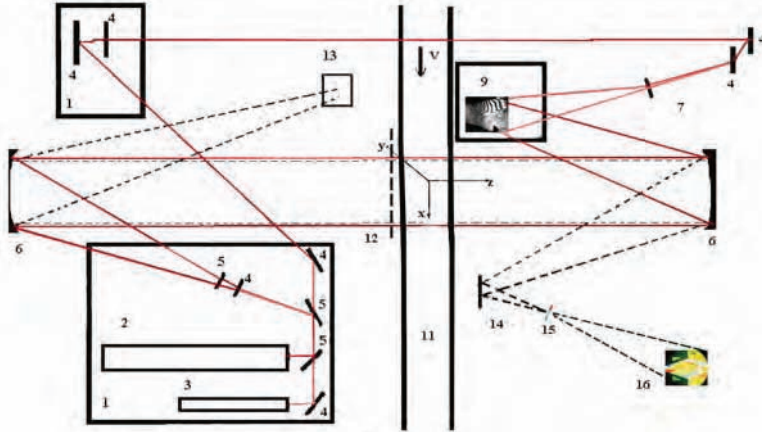


Fig. 23: The schema of the holographic interferometer/schlieren and shadow device in supersonic wind tunnel

6.3.2. Review of holographic interferograms

In order to demonstrate advantages of holographic interferometry in complex flow field testing, and compared with other classical methods, the series of experiments were performed in MTI supersonic and trisonic wind tunnel at flow velocity from $M_\infty = 0.7$ to 3.24. The photos of holographic interferograms illustrate this method. Figure 24 show some interferograms of different flow.

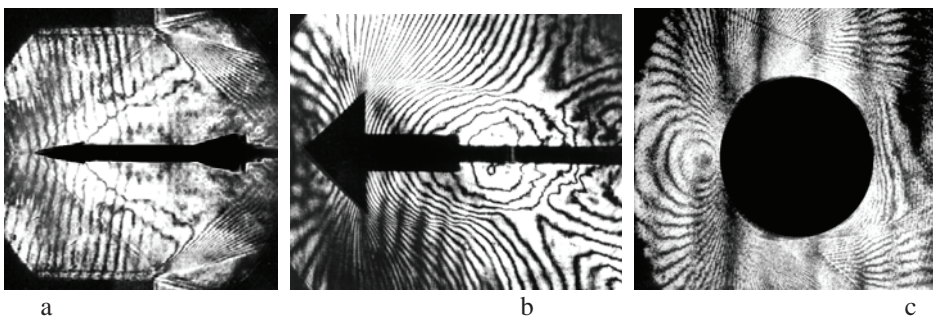


Fig. 24: Holographic interferogram of flow around missile for $M_\infty=1,56$ (a), cone 90° and $M_\infty=0,86$ (b) and 2D cylinder $M_\infty=0,76$ (flow is left to right)[31]

The usage of classical methods of nozzle flow field testing comprises the introduction of probe within the expansion region and holes perforation on nozzle surface. These interventions would significantly change the flow field. Optimization of this measurement is made by the holographic interferometry.

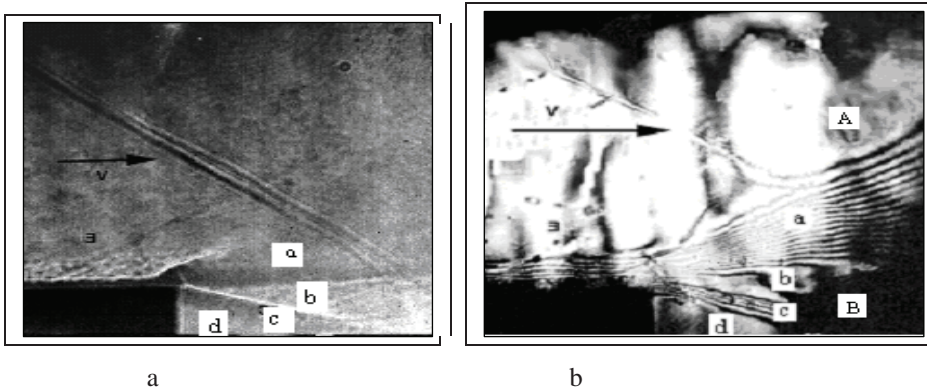


Fig. 25. Visualization of supersonic flow (left to right) around 2D 90° nozzle edge (Prandtl-Mayer expansion) $M_\infty=1,56$: a) shadow, and b) interferogram

In order to demonstrate and to compare complementary possibilities of optical methods in quantitative flow visualization, Prandtl-Mayer expansion tested by three optical methods is presented. Figure 25a,b and c show the flow visualization around 90° corner end edge for supersonic nozzle $M_\infty = 1,56$. The interferogram is recorded by double passing, collimated, object beam through the wind tunnel test section. The shadow is recorded on a holographic plate, because of collimated beams. The color schlieren is recorded in the same time with holographic interferogram.

The holographic interferograms were used for numerical calculation of flow field parameters in the vicinity of nozzle edge where the expansion fan is formed (fig. 25c). The fringe number N was read from this hologram. Points in front of expansion fan have $N=0$, since the last fringe has $N=17$. The theoretical and experimental values of Mach number in the expansion area are in good agreement $M_{exp} = 2.15$, $M_{the} = 2.13$ [5,29].

The photos in figure 26a and 26b present holographic interferograms of flow around sphere for $M_\infty=0.8$ (without shock wave) and $M_\infty=1,06$ (bow shock wave is in front of model). Fig. 26b is combination of holographic interferograms (upper part) and schlieren photo for the same flow. On the interferometric part of photo easily seen are: the stagnation point, the detached bow wave, the vortex sheet generated past sphere and so on.

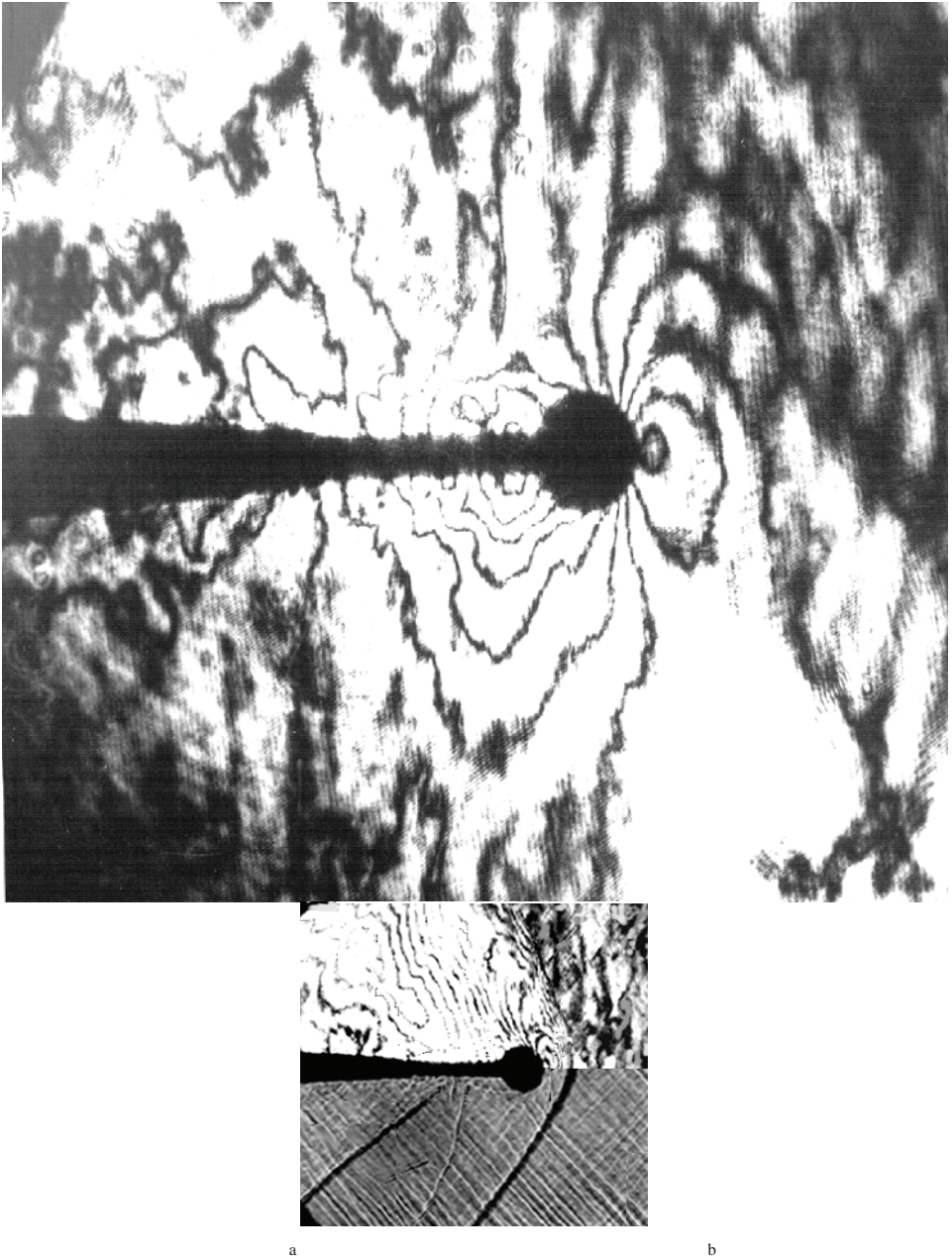


Fig. 26: Holographic interferogram of flow around sphere for $M_\infty = 0.82$ (a) and mix; hologram and schlieren for $M_\infty = 1.06$ (b)

Very interesting is example of flow visualization around tunnel wall perforations [5,30,32]. Many transonic tunnels are operated with perforated walls in the test section.

A number of investigations have been performed to determine how the flow in the test section is affected by the presence of the perforation. The next photos (Fig 27) reports on test performed in T-36, with a single slanted slot in the bottom plate of the test section. The disturbances originating from the slot are expressed by distortions of the parallel fringe system. A concentration of fringes indicated the formation of a pressure wave. The slanted slot was used because it had been reported that such geometry would considerably reduce the perturbation of free flow.

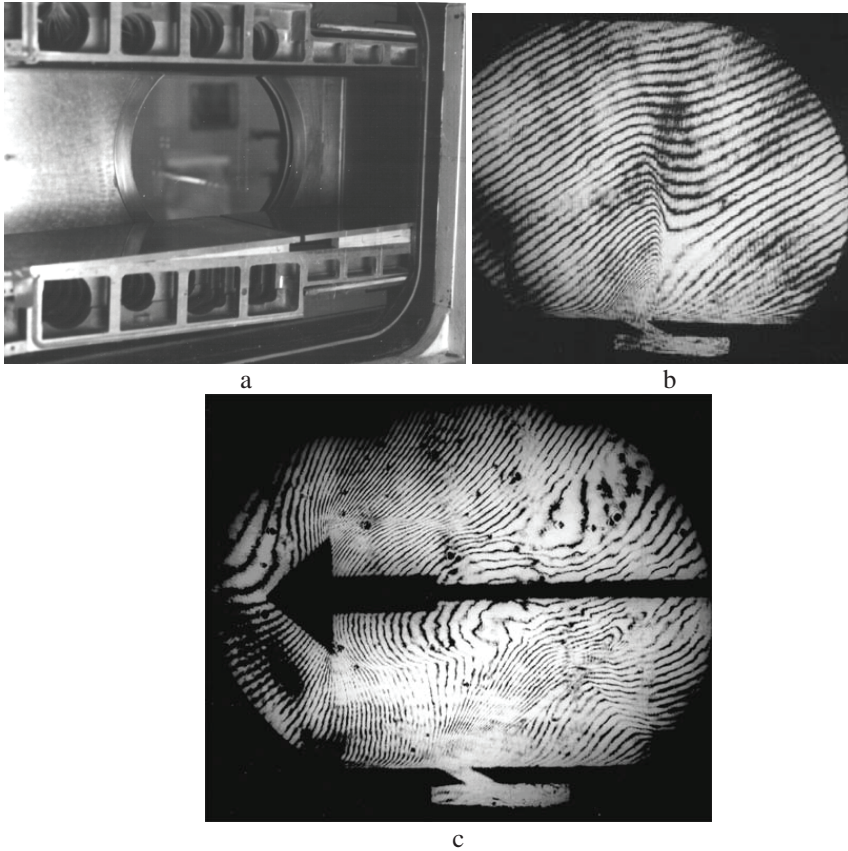


Fig. 27: Test section (a) and holographic interferograms of flow (flow is left to right) in the empty wind tunnel test section with wall perforation (slanted slot) (b) and with cone for $M_\infty = 0,83$ (c) [30]

The interferogram however shows that the disturbance from the slot is not at all negligible and reaches even beyond the axis of the test section (to about 60 % of the test section height). The perturbation has the influence on the model sting in the central line of the test section (fig 27c).

The interferograms of several supersonic racket nozzle configurations (fig. 28a) without and with different barriers are recorded in order to provide a good insight in the physical processes (figs. 28b,c,d). [5,7,31,36,37].

The theoretical value of Mach number in the output plane of the nozzle is estimated to be $M=2.6$. Using the data for pressure measurements, it is obtained $M=2.46$ and by means of holographic calculations, Mach number is $M=2.56$. The placing of barriers in the supersonic flow, leads to the appearance of the stagnation zone, shock and expansion waves. Visualization of the flow field made in the experiment indicates strong interaction of the turbulent boundary layer with the oblique shock wave in the divergent part of the nozzle.

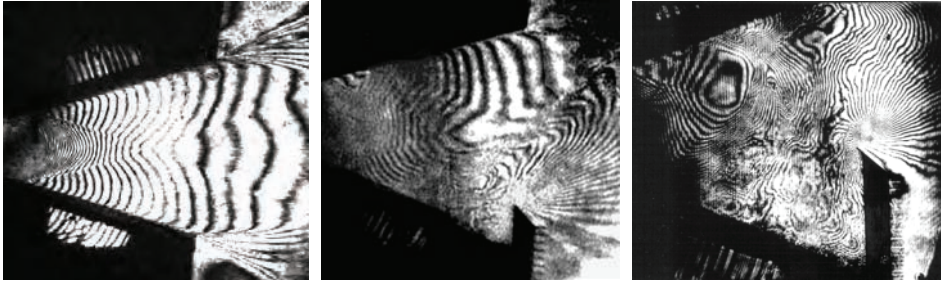


Fig. 28. Holographic interferograms for 2D supersonic nozzle without and with three barriers

Beside two-exposition method, there are used the real time method, the average or sandwich methods, the speckle interferometry, refraction interferometry, differential interferometry and so on. Optical holography use laser light in visible spectrum, and interferential effects are recorded on photo or thermosensitive emulsions. Electronic holography uses CCD cameras. In some specific cases acoustic and microwave holography, with electron beam, X – rays, or computer holography can be used. With similar possibilities, today are used speckle interferometry, moiré interferometry and shearography [1-5, 27,28].

6.4. Flow visualization by infrared thermography

Thermographic systems have been considered to analyse fluid-dynamic phenomena thirty years ago. Nowadays high resolution and differential infrared thermographic measurement systems open up new possibilities in it application [38,39]. Temperature field that can be measured by a thermographic system on the surface of a solid body invested by a flow is determined by a lot of combined effects. Very important effects are: conversion of kinetic energy of the flow into thermal energy, flow temperature variation in time and space, convection heat transfer phenomena between flow and body, conduction phenomena inside the body and radiation heat exchange of the body surface with surroundings. By correspondence between convective heat transfer coefficient and local turbulence it's possible to carry out information about the boundary layer. In addition to the laminar-to-turbulent transition boundary, the infrared camera was able to detect shock waves and present a time dependent view of the flow field. Figure 29 shows thermograms of tests have been performed using an high resolution thermographic system for fluid-dynamics analysis of a known test case, a wing profile, in a wind tunnel under variable and constant temperature condition at different air flow velocity[41,42].

A time dependent heat transfer code was developed to predict temperature distributions on the test subject and any necessary surface treatment. A commercially available infrared camera can be adapted for airborne use. Readily available infrared technology has the capability to provide detailed visualization of various flow phenomena in subsonic to hypersonic flight regimes.

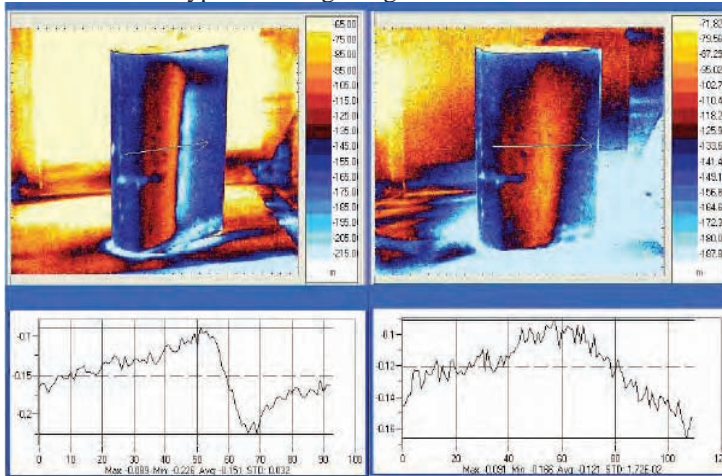


Fig. 29 Black aluminium airfoil with incidence of $7,5^\circ$ clockwise (a) and airfoil with incidence of $-7,5^\circ$ clockwise [42]

6.5. Computer Graphics Flow Visualization

Data originates from numerical simulations, such as those of computational fluid dynamics need to be analyzed by means of visualization to understand the flow. With the rapid increase of computational power for simulations, the demand for more advanced visualization methods has grown. Computer graphics flow visualization centers around visualization mapping, or the translation of physical flow parameters to visual representations. Starting from a set of standard mappings, a number of data preparation techniques is developed, to prepare the flow data for visualization [5,36,37,41].

The current strong demand for new flow visualization techniques, especially for large scale 3D numerical flow simulations, can only be satisfied by combining the efforts of fluid dynamics specialists, numerical analysts, and computer graphics experts. Additional knowledge is required from perceptual and cognitive psychology, and artists and designers can also contribute to this effort.

Conceptually, this process centers on visualization mapping or the translation of physical flow parameters to visual representations. Starting from a set of standard mappings partly based on equivalents from experimental visualization, a number of data preparation techniques is used, to prepare the flow data for visualization. Next, a number of perceptual effects and rendering techniques are described, and some problems in visual presentation are discussed. The paper ends with some concluding remarks and suggestions for future development.

Scientific visualization with computer-generated images can be generally divided on several stages:

- data generation: production of numerical data by measurement or numerical simulations

- data enrichment and enhancement: modification or selection of the data, to reduce the amount or improve the information content of the data.

- visualization mapping: translation of the physical data to suitable visual primitives and attributes.

- rendering: transformation of the mapped data into displayable images.

- display: showing the rendered images on a screen.

Test of the complex flow field (as the flow in the two dimensional supersonic nozzle with the deflector) by holographic interferometry, shows again the significant advantages of the holographic interferometry compared to shadow, schlieren and other classical ones. This method has special advantages when the complex flows are tested, e.g. flow around deflector, in the vicinity of the shock wave, etc.

Figure 30a shows numerical flow visualization of path line colored by velocity magnitude (m/s), for different times and $V_\infty=5.32$ m/s, around 2D hydrofoil in water tunnel [15]

Recently, flow visualization methods give the broad base for comparisons with numerical methods. The considered problem is very complex because both the Reynolds number and the Mach number influence the flow in the supersonic nozzle with deflector at the exit plane. An oblique shock wave and large region of separated flow are caused by the deflector (figs 28 and figs.31).

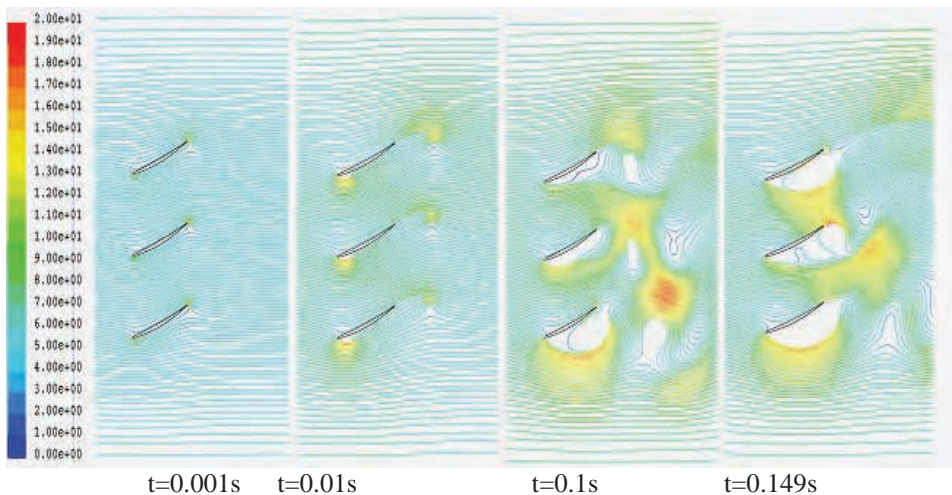


Figure 30: Numerical flow visualization of path line colored by velocity magnitude (m/s), for different times and $V_\infty=5.32$ m/s, around 2D hydrofoil in water tunnel [15].

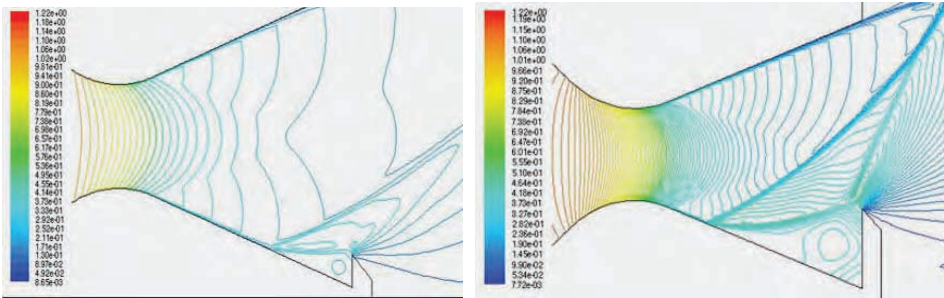


Fig.3.1

The complex two-dimensional supersonic flow in the nozzle with three deflectors at the exit is numerically simulated by the solution of the Reynolds-Averaged Navier-Stokes equations with a two-equation $k-\omega$ turbulent model. This model of turbulence is based on the Boussinesq approximation[36]

The used code captured main flow features and differences obtained with S-A and $k-\omega$ turbulence models are not substantial. It is shown that convergent results were obtained with all the meshes except the extra fine mesh.

7. CONCLUSION

This paper presents an overview of techniques for flow visualization. A brief introduction to experimental flow visualization methods is given. Every method is illustrated with photos of flow visualization effects. The advent of computer technique, new technology for illumination, modern and very powerful devices for digital image recording and processing make possible automatically analyze flow visualization effects and extract qualitative and quantitative information, which may not be readily available from conventional flow measurements. Experimental flow visualization is a starting point for numerical flow visualization of simulations using computer graphics. Parallel usage of experimental and numerical methods confirms the possibilities of numerical method application for complex flow analysis.

BIBLIOGRAPHY

1. W. Marzkirch,; Flow visualization, Academic Press, New York, 1977.
2. D.H. Stedman, G.R.Carignan : Flow Visualization II, 1981
3. W.J. Yang,; Flow visualization III proc. of 3. International Symposium, An Arbor MI, 1983, Hemisphere, New York, 1985.
4. G.S. Settles: Modern Developments in Flow Visualization, AIAA Journal, 24, 8, (1986), 1313-1323.
5. S. Ristic, Flow visualization techniques in wind tunnels- Non optical methods, Part I,II, Scientific Technical Review, Belgrade, LVII, 1,2 (2007), 39-51

6. Monografija VTI, 1996, Beograd
7. Z. Anastasijevic, S. Ristic : Review of Testing Possibilities in Experimental Aerodynamics Laboratory, Tehnika, Mašinstvo 55, (2006), 15-24
8. S. Ristic: Vizualizacija strujanja u aerotunelu pomoću TiCl₄, NTP, 39, 8, (1989), 8-14
9. L. Luo, & others, .Flowfield Around Ogive/Elliptic-Tip Cylinder at High Angle of Attack, AIAA J, 36, (1998), 1778-1787
10. LU F.K., G.S.Settles, Color Surface Flow Visualization of fine Generated Shock Wave Boundery Layer Interactions, Exper. in Fluids, 8, (1990), 352-356
11. S. RISTIC, P. Majstorović, Experimental investigation relative flow through model of straight profile grid., STR, 50, 6., (2000), 29-36
12. J.C. McDaniel, R.K. Hanson, Qualitative Planer Visualization in Gaseous Flow Field Using Laser Indused Fluorescent, Flow Visualization III, (1983), 113
13. M. Havermann , J. Haertig , C. Rey , and A. George : Application of Particle Image Velocimetry to High-Speed Supersonic Flows in a Shock Tunnel French-German Research Institute of Saint-Louis (ISL), 5 Rue du Général Cassagnou, F-68301 Saint-Louis, France, 1999
14. Puharić M. , S. Ristic., Kutin M., Adamović Z., Laser Doppler Anemometry in Hydrodynamic Testing, Journal of Russian Laser Research, 28, 6, (2007), 619-628
15. S. Ristic, Laser Doppler Anemometry and its Application in Wind Tunnel Tests, Scientific Technical Review, 62,3-4, (2007), 64-75
16. J.R.Growder, Fluorescent Mini Tufts For Flow Visualization On Rotating surfaces, Flow Visualization III, 3th international symposium on flow visualization, sept. 6-9, An Arbor Michigan USA, (1983), 55-64
17. G. Ocokoljića, J. Radulović, Flow visualization and aerodynamical coefficients determination for the LASTA-95 model in wind tunnel T-35., STR, n.2, (2006), 63-69
18. S. Ristic, Vizualizacija podzvučnog strujanja metodom fluorescentnih končića, Jubilarni broj NTP-a, 46, 4-5, (1996), 73-76
19. D. Damljanović, S. Ristic., Eksperimentalno ispitivanje aerodinamičkih karakteristika modela laserski vođene bombe, VTG, br. 5, (2005), 406-417
20. S. Ristić., D. Matić, A. Vitić.: Determination of aerodynamical coefficients and visualization of the flow around the axisymetrical model by experimental and numerical methods, STR, 55, 3-4, (2005), 42-49
21. S. Ristic, D. Matić, A. Vitić., Samardžić, M.: *The numerical and experimental testing of the axisymmetric model flow*, Facta Universitatis Series Mechanics, Automatic Control and Robotics, 5, 1, (2006), 145-152
22. S. Ristic.: Optimizacija primene uljanih premaza u vizualizaciji strujanja u aerotunelima, 2005., Tehnika, god LX. n.5, Elektrotehnika 54, 5, (2005), 8-14
23. S. Ristic, J. Isaković, M. Srećković, D. Matić, Comparative analysis of experimental and numerical flow visualization, FME Transactions, 34, (2006), 143-149
24. S. Ristic, Optical methods in wind tunnel flow visualization, FME Transactions, 34, (2006), 7-13
25. B. Song, Experimental and Numerical Investigations of Optimized High-Turning Supercritical Compressor Blades, Dissertation, Faculty of the Virginia Polytechnic Institute and State University, November 2003, Blacksburg, Virginia

26. S. Ristic, Premazi osetljivi na pritisak, nova mogućnost vizualizacije strujanja, VTG, 1, 2006, 35-48.
27. C.M. Vest, Holographic Interferometry, New York, Wiley and sons, 1982.
28. D.W. Watt, C.M. Vest, Digital Interferometry for Flow Visualization, Exper. in Fluids, 5, (1987), 401-405
29. S. Ristic, Testing of the Flow Field Around the Nozzle Edge Using the Method of Holographic Interferometry, Fizika, 22, 3, (1990), 529-543
30. S. Ristic, Disturbance of Transonic wind Tunnel Flow by a Slot in the Tunnel Wall, Experiments in fluids, 11, (1990), 403-405
31. S. Ristic, Optimizacija kvantitativne obrade holografskih interferograma za 2D i osno simetrična strujanja, Jubilarni broj NTP-a, 46, 4-5, (1996) 37-45
32. S. Ristic, M. Srećković, Pressure Disturbances Testing by Schlieren Method and Holographic Interferometry, Laser '98, 7-11, Tucson, Arizona, Proceedings, (1998), 568-547
33. S. Milićev, D. Pavlović, S. Ristic, A. Vitić, On the Influence of Spike Shape at Supersonic Flow Past Blunt Bodies, 2002, Facta universitatis, series: Mechanics, Automatic, Control and Robotics, 3, 12, 371-382
34. S. Ristić, Srećković M., Testing of supersonic wind tunnel flow by holographic interferometry, Atti dela Fondazione Giorgio Ronchi, 61, (2006), 231-240
35. S. Ristic, Z. Anastasijevic, J. Isakovic, New Combined Holographic Interferometer and Schlieren Device for Wind Tunnel T-38, proceedings of ICASAT 2007, Tripoli 23-25/04/2007
36. S. Ristic, M. Kozic, Experimental and numerical investigation of flow separation in a supersonic nozzle, *Journal of Russian Laser Research*, 29, 4, (2008), .377- 389
37. S. Ristic, M. Kozic, Optical and numerical visualization in analysis of deflector angle influence on 2d supersonic nozzle flow, B06, 2nd International Congress of Serbian Society of Mechanics, 1-5 June 2009, Palić (Subotica), Serbia
38. D. W. Banks, C. P. van Dam and H. J. Shiu, G. M. Miller, Visualization of In-Flight Flow Phenomena Using Infrared Thermography, NASA/TM-2000-209027
39. [dhttp://www.aivela.org/Salviuolo_paper06.pdf](http://www.aivela.org/Salviuolo_paper06.pdf)
40. Q. Xia Tsa and H.M. Papamoschou, Numerical Investigation of Supersonic Nozzle Flow Separation, AIIA, 29995, no. 4640 D.
41. R.L. Roe, Numerical Methods in Aeronautical Fluid Dynamics, London, Academic Press, 1982

VIZUALIZACIJA STRUJANJA – POGLED U NEVIDLJIVO

Slavica Ristić

Vizualizacija strujanja je veoma značajna oblast u eksperimentalnoj i kompjuterskoj dinamici fluida i dugi niz godina je predmet istraživanja. U ovom radu su prikazane izabrane tehnika vizualizacije strujanja. Opisani su osnovni fizički principi ovih metoda, kao i njihova primena u vizualizaciji podzvučnih, okozvučnih i nadzvučnih strujanja u aerodinamičkim i vodenim tunelima: metode sa direktno ubacivanjem markera (dim, boje, magla, različite male čestice), gasni i hidrogenski mehurići, vizualizacija strujanja sa končićima, sa uljanim emulzijama, tečnim kristalima, bojama osetljivim na promenu temperature i pritiska, optičkim metodama kao što su metod senke, šliren, holografska interferometrija, Laser Doppler anemometrija, anemometrija za merenje vektora brzine mikroskopskih čestica u fluidu, pomoću njihovih slika i drugih specijalnih tehnika. Skoro sve prikazane slike su snimljene u laboratorijama Vojnotehničkog instituta u Beogradu.

Ključne reči: vizualizacija strujanja, aerodinamički tunnel, vodeni tunnel, optičke metode, LDA PIV